Asociación Argentina
de Mecánica Computacional

Mecánica Computacional Vol XXXI, págs. 3387-3396 (artículo completo)
Alberto Cardona, Paul H. Kohan, Ricardo D. Quinteros, Mario A. Storti (Eds.)
Salta, Argentina, 13-16 Noviembre 2012

SIMULATION OF CARBON DIOXIDE STORAGE APPLYING ACCURATE PETROPHYSICS, FLUID-FLOW AND SEISMICS MODELS

Gabriela B. Savioli[a], Juan E. Santos[b], José M. Carcione[c] and Davide Gei[c]

[a]*Laboratorio de Ingeniería de Reservorios, Instituto del Gas y del Petróleo and Dto. de Ing. Química, Facultad de Ingeniería, Universidad de Buenos Aires, Av. Las Heras 2214 Piso 3 C1127AAR Buenos Aires, Argentina, gsavioli@di.fcen.uba.ar*

[b]*CONICET, Instituto del Gas y del Petróleo, Facultad de Ingeniería, Universidad de Buenos Aires and, Universidad de La Plata and, Department of Mathematics, Purdue University, 150 N. University Street, West Lafayette, Indiana, 47907-2067, USA, santos@math.purdue.edu*

[c]*Istituto Nazionale di Oceanografia e di Geofisica Sperimentale (OGS), Borgo Grotta Gigante 42c, 34010 Sgonico, Trieste, Italy jcarcione@inogs.it*

Keywords: CO_2 Sequestration, Finite Elements, Wave Propagation

Abstract. Capture and storage of Carbon dioxide in aquifers and reservoirs is one of the solutions to mitigate the greenhouse effect. Geophysical methods can be used to monitor the location and migration of the gas in the underground. To perform this task properly, a suitable geological model is important, which simulates the geometry and petro-elastical properties of the different formations. In this work we integrate numerical simulators of CO_2-brine flow and seismic wave propagation to model and monitor CO_2 storage in saline aquifers. We also build a petrophysical model of a shaly sandstone based on porosity and clay content and considering the variation of properties with pore pressure and fluid saturation. The pressure map before the injection of CO_2 is assumed to be hydrostatic for which a reference porosity map is defined. The permeability is assumed to be anisotropic and is obtained from first principles as a function of porosity and grain sizes. The density is the usual arithmetic average of the sandy and shaly components. The numerical simulator of the CO_2-brine flow is based on the Black-Oil formulation for two phase flow in porous media, which uses the Pressure-Volume-Temperature (PVT) behavior as a simplified thermodynamic model. The propagation of waves in porous media is described using a viscoelastic model that takes into account the dispersion and attenuation effects due to the presence of heterogeneities in the fluid and solid phase properties. We introduce the P-wave attenuation following White's model of porous layers alternately saturated with brine and CO_2. S-wave attenuation is considered with a mechanism related to the P-wave one. Numerical examples of CO_2 injection and time-lapse seismics in the Utsira formation at the Sleipner field are analyzed. The Utsira formation is represented using the new petrophysical model that allows a realistic inclusion of shale seals and fractures. The results of the simulations show the capability of the proposed methodology to monitor the migration and dispersal of the CO_2 plume and to make long term predictions.

1 INTRODUCTION

Geologic storage of CO_2 consists in injecting the gas into a geologic formation at depths typically greater than 1000 m, where it is present at supercritical conditions (Arts et al., 2008). Saline aquifers are suitable as storage sites due to their large volume and their common occurrence in nature.

In the Sleipner gas field (North Sea), the first industrial scale CO_2 injection project is being developed (Chadwick et al., 2005). CO_2 separated from natural gas produced at Sleipner is currently being injected into the Utsira Sand, a saline aquifer some 26000 km^2 in area.

Numerical modeling of CO_2 injection and seismic monitoring are important tools to understand the behavior of CO_2 after its injection and to make long term predictions. To perform this task properly, a reliable geological model is important, which simulates the geometry and petroelastical properties of the different formations. This model assumes a shaly sand, which represents the Utsira Sand or shale formation, depending on the clay content. The permeability is assumed to be anisotropic and is obtained from first principles as a function of porosity and grain sizes.We generate the geological model from the initial porosity (at hydrostatic pore pressure) and clay content. The simultaneous flow of brine and CO_2 is modeled with the Black-Oil formulation for two-phase flow in porous media (Aziz and Settari, 1985). After injection, the CO_2 migrates upwards, accumulating below thin shale (mudstone) layers. These layers allow the vertical CO_2 migration to the top because they are not fully sealing. The fluid pressures and saturations computed by the fluid simulator are used to obtain the properties of the CO_2 at in-situ conditions and the petro-physical properties of the Utsira Sand. These are obtained with White mesoscopic model (Carcione, 2007).

Wave propagation is based on a viscoelastic model that considers dispersion and attenuation effects. In regions with partial CO_2 saturation, following White's theory (White et al., 1975), we consider P-wave attenuation due to wave-induced fluid flow at mesoscopic scales using a model of porous layers alternately saturated with brine and CO_2. The results of the flow simulator allow us to determine the phase velocities and attenuation coefficients of P and S waves at each computational cell using White's model.

The numerical examples present simulations of CO_2 injection and time-lapse seismograms in the Utsira Sand aquifer at Sleipner field. We build a petrophysical model of the Utsira formation based on porosity and clay content and taking into account the variation of properties with pore pressure and CO_2 saturation. This model is able to simulate embedded mudstone layers of very low permeability that accumulate CO_2 but also allow its migration. The proposed methodology is able to identify the spatio-temporal distribution of CO_2 after its injection. Attenuation and dispersion effects are clearly observed in the snapshots and the recorded traces. This methodology allowed us to identify the horizontal and vertical saturation distribution of CO_2 over long periods of time.

2 PETROPHYSICAL MODEL OF THE UTSIRA FORMATION

The petrophysical model assumes a shaly sand and is generated from the initial porosity ϕ_0 (at hydrostatic pore pressure p_H) and clay content C.

The pressure dependence of properties is based on the following relationship between poros-

ity and pore pressure p,

$$\frac{(1-\phi_c)}{K_s}(p-p_H) = \phi_0 - \phi + \phi_c \ln\frac{\phi}{\phi_0}, \tag{1}$$

where ϕ_c is a critical porosity.

The bulk modulus of the dry matrix is estimated from the pressure dependent porosity using the Krief equation (Carcione et al., 2006),

$$K_m = K_s(1-\phi)^{A/(1-\phi)}, \tag{2}$$

where the bulk modulus of the solid grains K_s is the arithmetic average of the Hashin-Shtrikman upper and lower bounds. The rock is formed with quartz (bulk modulus of 40 GPa) and clay (bulk modulus of 15 GPa).

We assume the grain to be a Poisson medium, then the shear modulus of the solid grains is $\mu_s = 3K_s/5$ and we set

$$\mu_m = \mu_s(1-\phi)^{A/(1-\phi)}. \tag{3}$$

The black-oil simulator needs the compressibility C_{pp} defined by Zimmerman et al. (1986), which is given by

$$C_{pp} = \frac{1}{\phi}\left(\frac{1}{K_m} - \frac{1+\phi}{K_s}\right) \tag{4}$$

As permeability is anisotropic, we consider horizontal permeability κ_x and vertical permeability κ_z. Carcione et al. (2000) derived a model depending on porosity and clay content, assuming that a shaly sandstone is composed of a sandy matrix and a shaly matrix with partial permeabilities

$$\kappa_q = \frac{R_q^2\phi^3}{45(1-\phi)^2(1-C)} \quad \text{and} \quad \kappa_c = \frac{R_c^2\phi^3}{45(1-\phi)^2 C} \tag{5}$$

where R_q and R_c denote the average radii of sand and clay particles, respectively.

Therefore, the average permeability of the shaly sandstone along the horizontal direction is given by

$$\frac{1}{\kappa_z} = \frac{1-C}{\kappa_q} + \frac{C}{\kappa_c} \tag{6}$$

Following Carcione et al. (2003) , we assume

$$\frac{\kappa_x}{\kappa_z} = \frac{1-(1-0.3a)\sin\pi S_w}{a(1-0.5\sin\pi S_w)}, \tag{7}$$

where a is a permeability-anisotropy parameter and S_w is the brine saturation.

Note that for $S_w = 0$ or 1, $\kappa_z = a\kappa_x$. It is $\kappa_x > \kappa_z$ at full water saturation, due to pore cross sections which are larger in the x-direction.

As water saturation is reduced, and the larger pores drained first, a saturation is reached at which $\kappa_x = \kappa_z$. Then, as saturation is further reduced, $\kappa_x < \kappa_z$. At the other end (full gas saturation), we have again $\kappa_x > \kappa_z$.

3 THE BLACK-OIL FORMULATION OF TWO-PHASE FLOW IN POROUS MEDIA

The simultaneous flow of brine and CO_2 in porous media is described by the well-known Black-Oil formulation applied to two-phase, two component fluid flow (Aziz and Settari, 1985). In this way, CO_2 component may dissolve in the brine phase but the brine is not allowed to vaporize into the CO_2 phase. The differential equations, obtained by combining the mass conservation equations with Darcy's empirical law, are

$$\nabla \cdot (\underline{\kappa}(\frac{k_{rCO2}}{B_{CO2}\eta_{CO2}}(\nabla p_{CO2} - \rho_{CO2} g \nabla D) + \frac{R_s k_{rb}}{B_b \eta_b}(\nabla p_b - \rho_b g \nabla D))) + \frac{q_{CO2}}{\rho^{SC}_{CO2}} = \frac{\partial\Big[\phi\left(\frac{S_{CO2}}{B_{CO2}} + \frac{R_s S_b}{B_b}\right)\Big]}{\partial t}, \tag{8}$$

$$\nabla \cdot (\underline{\kappa}\frac{k_{rb}}{B_b \eta_b}(\nabla p_b - \rho_b g \nabla D) + \frac{q_b}{\rho^{SC}_b} = \frac{\partial\Big[\phi\frac{S_b}{B_b}\Big]}{\partial t}. \tag{9}$$

Subscripts $\beta = b, CO2$ denote brine and CO_2 phases, respectively. The unknowns for the Black-Oil model are the fluid pressures p_β and saturations S_β. Also ρ_β is density, q_β mass rate of injection per unit volume, and the funcions $k_{r\beta}$ and η_β are the relative permeability and viscosities, respectively. Finally $\underline{\kappa}$ is the absolute permeability tensor and ϕ is porosity.

The Black-Oil formulation uses as a simplified thermodynamic model, the PVT data R_s and B_β defined as

- $R_s = \frac{V^{SC}_{dCO2}}{V^{SC}_b}$, CO_2 solubility in brine;
- $B_{CO2} = \frac{V^{res}_{CO2}}{V^{SC}_{CO2}}$, CO_2 formation volume factor;
- $B_b = \frac{(V^{res}_{dCO2} + V^{res}_b)}{V^{SC}_b}$, brine formation volume factor;

with V^{res}_{CO2}, V^{res}_b and V^{res}_{dCO2} the volume of CO_2, brine and dissolved CO_2 in brine at reservoir conditions; and V^{SC}_{CO2}, V^{SC}_b and V^{SC}_{dCO2} are the volume of CO_2, brine and dissolved CO_2 in brine at standard conditions, respectively. Also, ρ^{SC}_b and ρ^{SC}_{CO2} are the CO_2 and brine densities at standard conditions.

R_s and B_b can be expressed in terms of the equilibrium properties obtained from an equation of state:

- $R_s = \frac{\tilde{\rho}^{SC}_b \chi_{CO2}}{\tilde{\rho}^{SC}_{CO2}(1 - \chi_{CO2})}$
- $B_b = \frac{\rho^{SC}_b}{\rho_b(1 - \omega_{CO2})}$

The conversion from compositional data from equations of state into the Black-Oil PVT data is performed applying an algorithm developed by Hassanzadeh et al. (2008) which uses the brine and CO_2 molar density at standard conditions; and the CO_2 mole and mass fraction in the brine phase.

Two algebraic equations relating the saturations and pressures complete the system:

$$S_b + S_{CO2} = 1, \qquad p_{CO2} - p_b = P_C(S_b), \tag{10}$$

where P_C is the capillary pressure.

The numerical solution was obtained employing the public domain software BOAST (Fanchi, 1997). BOAST solves the differential equations using IMPES (IMplicit Pressure Explicit Saturation), a semi-implicit finite difference technique (Aziz and Settari, 1985).

4 A VISCOELASTIC MODEL FOR WAVE PROPAGATION

The propagation of waves in fluid-saturated porous media is described using an equivalent viscoelastic model that takes into account the dispersion and attenuation effects due to the presence of heterogeneities in the fluid and solid phase properties.

The equation of motion in a 2D isotropic viscoelastic domain Ω with boundary $\partial\Omega$ can be stated in the space-frequency domain as

$$-\omega^2 \rho u - \nabla \cdot \sigma(u) = f(x,\omega), \quad \Omega \tag{11}$$

$$-\sigma(u)\nu = i\omega \mathcal{D} u, \quad \partial\Omega, \tag{12}$$

where $u = (u_x, u_y)$ is the displacement vector. Here ρ is the bulk density and (12) is a first-order absorbing boundary condition using the positive definite matrix $\mathcal{D}$, which definition is given in (Ha et al., 2002).

The stress tensor $\sigma(u)$ is defined in the space-frequency domain by

$$\sigma_{jk}(u) = \lambda_G(\omega)\nabla \cdot u\delta_{jk} + 2N(\omega)\varepsilon_{jk}(u), \quad \Omega, \tag{13}$$

where $\varepsilon_{jk}(u)$ denotes the strain tensor and δ_{jk} is the Kroenecker delta.

The coefficient N in (13) is the shear modulus of the dry matrix, while the Lamé coefficient is $\lambda_G = K_G - \frac{2}{3}\mu$ in 3D and $\lambda_G = K_G - \mu$ in 2D. K_G is the Gassmann's undrained bulk modulus, computed as follows:

$$K_G = K_m + \alpha^2 K_{av}$$

$$\alpha = 1 - \frac{K_m}{K_s},$$

$$K_{av} = \left[\frac{\alpha - \phi}{K_s} + \frac{\phi}{K_f}\right]^{-1}.$$

where

- K_m: bulk modulus of the dry matrix
- K_s: bulk modulus of the solid grains
- K_f: bulk modulus of the saturant fluid

Following (White et al., 1975), we consider P-wave attenuation due to wave induced fluid flow at mesoscopic scale using a model of porous layers alternately saturated with brine and CO_2 respectively. This approach yields a complex and frequency dependent P-wave modulus $E(\omega) = lambda_G(\omega) + 2N(\omega)$ for the formation. Recall that in a viscoelastic solid, the phase velocity and quality factor $Q(\omega)$ are defined by the relations

$$v_p(\omega) = \left[\mathrm{Re}\left(\frac{1}{vc_p(\omega)}\right)\right]^{-1}, \qquad Q(\omega) = \frac{\mathrm{Re}(vc_p(\omega)^2)}{\mathrm{Im}(vc_p(\omega)^2)}, \tag{14}$$

where $vc_p(\omega)$ is the complex and frequency dependent compressional velocity defined as

$$vc_p(\omega) = \sqrt{\frac{E(\omega)}{\rho}}. \tag{15}$$

S-wave attenuation is also taken into account making the shear modulus complex an frequency dependent using another relaxation mechanism related to the P-wave mechanism (Carcione et al., 2012).

The approximate solution of (11) with the boundary conditions (12) is obtained using an iterative finite element domain decomposition procedure. To approximate each component of the solid displacement vector we employed the nonconforming finite element space defined in (Douglas, Jr. et al., 1999), since it generates less numerical dispersion than the standard bilinear elements (Zyserman et al., 2003). It can be demonstrated that the error associated with this numerical procedure measured in the energy norm is of order h (Ha et al., 2002), where h is the size of the computational mesh.

5 MODEL OF THE UTSIRA FORMATION AND CO_2 INJECTION.

We consider a 2D model of the Sleipner field constructed using an initial porosity at hydrostatic pressure and the clay content of the formation. The model has 400 m thickness (top at 700 m and bottom 1100 m b.s.l.). Within the formation, there are several mudstone layers which act as barriers to the vertical motion of the CO_2 and can be observed in Figure 1 . The viscosity, density and bulk modulus of CO_2 were obtained from the Peng-Robinson equations as a function of temperature and pore pressure (Hassanzadeh et al., 2008).

CO_2 is injected at a constant flow rate of one millon tons per year. The injection point is located at the bottom of the Utsira formation: $x = 600$ m, $z = 1060$ m. Figure 2 shows the saturation field after 2 years (left) and 4 years (right) of CO_2 injection, computed using the BOAST flow simulator.

Figure 3 displays the spatial distribution of P-wave phase velocity v_p (left) and attenuation coefficient $1000/Q_p$ (rigth) at 75 Hz after 2 years of CO_2 injection. It can be observed a decrease in P- wave velocity in zones of CO_2 accumulation and a corresponding increase in attenuation.

6 TIME-LAPSE SEISMIC MONITORING

To analyze the capability of seismic monitoring to identify zones of CO_2 accumulation, the media is excited with a compressional point source located at $x = 600$ m, $z = 710$ m before and after 2 and 4 years of CO_2 injection. Time histories measured near the surface are shown in Figures 4 before (left) and after 2 years (right) of CO_2 injection. Figure 5 shows time histories after 2 (left) and 4 (right) years of CO_2 injection, respectively.

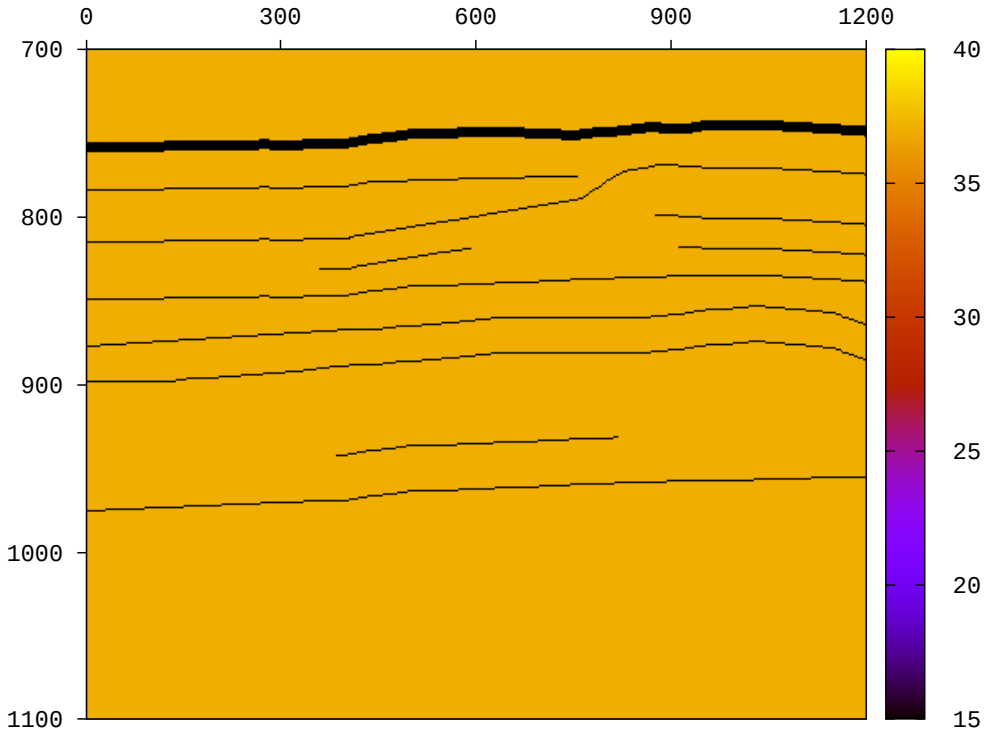

Figure 1: Porosity map

The upper reflection in Figures 4 and 5 is due to the direct wave coming from the point source. The lower reflection in Figures 4 (right) and 5 is due to the CO_2 accumulations below the deepest mudstone layer.

Figure 5 (right) shows another reflection due to the upper accumulation, which appears in the right side. Finally, Figure 6 displays the traces measured at x= 750 m, z = 710 m shown in Figure 4 .

7 CONCLUSIONS

In this work we integrate numerical simulators of CO_2-brine flow and seismic wave propagation to model and monitor CO_2 storage in saline aquifers. We also build a petrophysical model of a shaly sandstone based on porosity and clay content and considering the variation of properties with pore pressure and fluid saturation. Numerical examples show the effectiveness of this metodology to detect the spatio-temporal distribution of CO_2. Therefore, it constitutes an important tool to monitor the migration and dispersal of the CO_2 plume and to make long term predictions.

8 AKNOWLEDGEMENTS

This work was partially funded by CONICET, Argentina (PIP 0952) and Universidad de Buenos Aires (UBACyT 20020090100131)

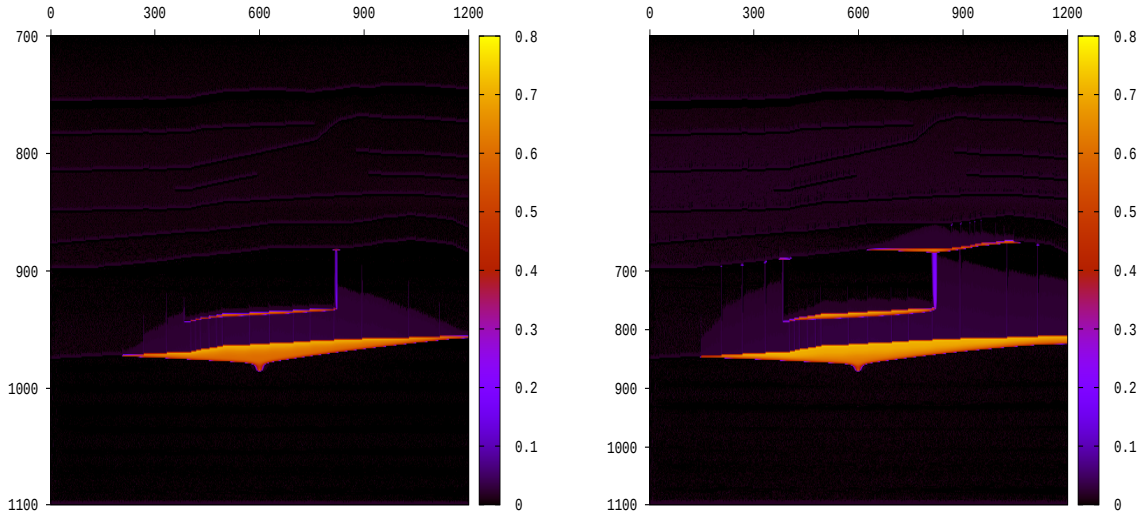

Figure 2: CO_2 saturation distribution after 2 years (left) and 4 years of injection. The injection point is located at x= 600 m, z= 1060 m

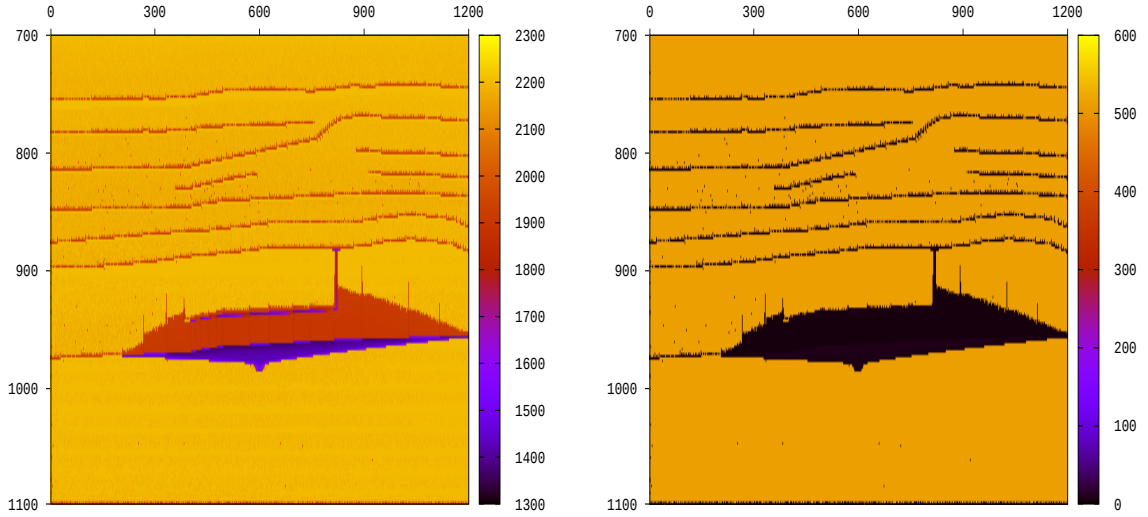

Figure 3: P-wave phase velocity v_p (left) and attenuation coefficient $1000/Q_p$ (right) after 2 years of CO_2 injection

REFERENCES

Arts R., Chadwick A., Eiken O., Thibeau S., and Nooner S. Ten years of experience of monitoring CO_2 injection in the utsira sand at sleipner, offshore norway. *First break*, 26:65–72, 2008.

Aziz K. and Settari A. *Petroleum Reservoir Simulation*. Elsevier Applied Science Publishers, Great Britain, 1985.

Carcione J., Gei D., Picotti S., and Michelini A. Cross-hole electromagnetic and seismic modeling for co2 and monitoring in a saline aquifer. *Journal of Petroleum Science and Engineering*, 2012. In press.

Carcione J., K. H., and Helle H.B. Effects of pressure and saturating fluid on wave velocity and attenuation of anisotropic rocks. *Int.J. Rock Mech. Min. Sci.*, 40:389–403, 2003.

Carcione J.M. *Wave fields in real media: Wave propagation in anisotropic, anelastic, porous*

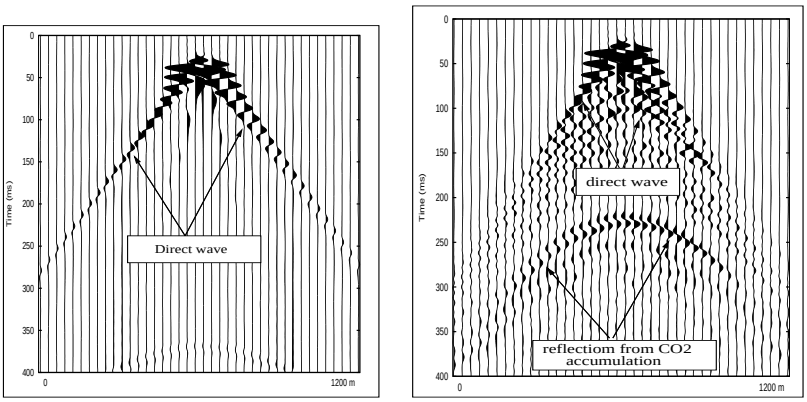

Figure 4: Traces of the z-component of the displacement before (left) and after 2 years (right) CO_2 injection. The upper reflection is due to the direct wave coming from the point source. The second reflection is due to the deepest CO_2 accumulation

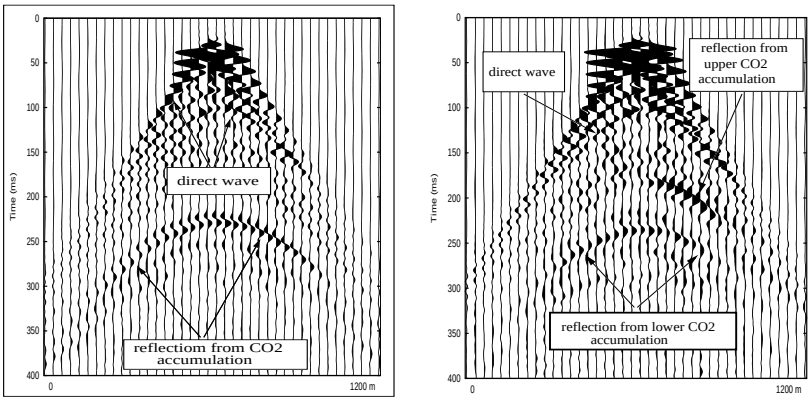

Figure 5: Traces of the z-component of the displacement after 2 years (left) and 4 years (right) of CO_2 injection. The lower reflection is due to the deepest CO_2 accumulation. The earlier reflection to the right is due to the upper CO_2 accumulation

and electromagnetic media, volume 38 of *Handbook of Geophysical Exploration*. Elsevier, 2nd edition, revised and extended, 2007.

Carcione J.M., Gurevich B., and Cavallini F. A generalized Biot-Gassmann model for the acoustic properties of shaley sandstones. *Geophysical Prospecting*, 48:539–557, 2000.

Carcione J.M., Picotti S., Gei D., and Rossi G. Physics and seismic modeling for monitoring CO_2 storage. *Pure and Applied Geophysics*, 163:175–207, 2006.

Chadwick A., Arts R., and Eiken O. 4d seismic quantification of a growing CO_2 plume at sleipner, north sea. *Dore A G and Vincent B (Eds) Petroleum Geology: North West Europe and Global Perspectives - Proc. 6th Petroleum Geology Conference*, pages 1385–1399, 2005.

Douglas, Jr. J., Santos J.E., Sheen D., and Ye X. Nonconforming Galerkin methods based on quadrilateral elements for second order elliptic problems. *RAIRO Mathematical Modelling and Numerical Analysis (M2AN)*, 33:747–770, 1999.

Fanchi J. *Principles of Applied Reservoir Simulation*. Gulf Professional Publishing Company, Houston, Texas, 1997.

Ha T., Santos J.E., and Sheen D. Nonconforming finite element methods for the simulation of waves in viscoelastic solids. *Comput. Meth. Appl. Mech. Engrg.*, 191:5647–5670, 2002.

Hassanzadeh H., Pooladi-Darvish M., Elsharkawy A., Keith D., and Leonenko Y. Predicting

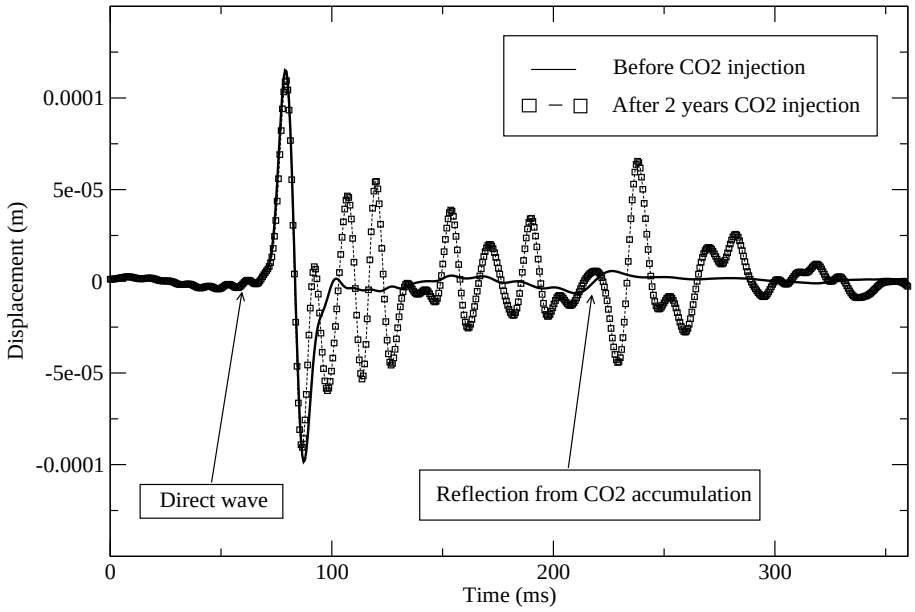

Figure 6: Traces of particle velocity of the solid phase before and after 2 years of CO_2 injection.

PVT data for CO_2-brine mixtures for black-oil simulation of CO_2 geological storage. *International Journal of Greenhouse Gas Control*, 2:65–77, 2008.

White J.E., Mikhaylova N.G., and Lyakhovitskiy F.M. Low-frequency seismic waves in fluid-saturated layered rocks. *Izvestija Academy of Siences USSR, Physics of Solid Earth*, 10:654–659, 1975.

Zimmerman R.W., H. S.W., and King M.S. Compressibility of porous rocks. *Journal of Geophysical Research*, 91:12765–12777, 1986.

Zyserman F.I., Gauzellino P.M., and Santos J.E. Dispersion analysis of a non-conforming finite element method for the Helmholtz and elastodynamic equations. *Int. J. Numer. Meth. Engng.*, 58:1381–1395, 2003.